Forest Ecology and Management 612 (2026) 123742

Contents lists available at ScienceDirect

Forest Ecology and Management

journal homepage: www.elsevier.com/locate/foreco

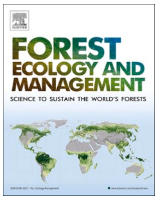

Forest structure from airborne laser scanning explains nationwide occurrence patterns of pine marten, stoat and least weasel across Finland

Pinja-Emilia Lämsä [a,*], Aarne Hovi [a], Andreas Lindén [b], Miina Rautiainen [a]

[a] School of Engineering, Aalto University, Espoo, Finland
[b] Natural Resources Institute Finland (Luke), Helsinki, Finland

ARTICLE INFO

Keywords:
Lidar
Forest structure
Occupancy modelling
Remote sensing
Mustelids

ABSTRACT

Forest structural complexity strongly influences habitat suitability for forest-dwelling species. Airborne laser scanning (ALS) provides efficient nationwide quantification of three-dimensional forest structure, but its applications in animal ecology remain limited, particularly for understudied mustelids. Here, we combined nationwide ALS data from 173 flight campaigns with species presence-absence observations, an unprecedented scale for mustelid studies, to assess how ALS-derived forest structural metrics predict the occurrence of pine marten, stoat, and least weasel in Finland. We modeled occurrences using spatial hierarchical generalized linear mixed-effects models. ALS metrics capturing vertical complexity and canopy cover, alongside landscape and climate variables, explained broad-scale habitat associations for pine marten and stoat. Least weasel occurrence was less predictable, likely reflecting its microhabitat preferences and dependence on voles. Key predictors of mustelid occurrence included canopy height variability, mid- and upper-canopy density, and canopy cover of tree layer. Our findings show that nationwide ALS combined with species occurrence data can reveal habitat preferences of small and medium-sized mustelids, supporting conservation, monitoring and management planning.

1. Introduction

Forests are structurally complex environments, that can be vertically stratified into distinct layers with differences in composition, light availability, and microclimatic conditions, thereby influencing habitat suitability for a wide range of forest dwelling animal species (McElhinny et al., 2005). Stratification may include the canopy layer, formed by the crowns of mature trees; the subcanopy and shrub layer, consisting of smaller trees and tall shrubs, and an understory or ground layer, dominated by herbaceous plants, mosses and woody saplings. Understory vegetation and complex canopy structures provide shelter, prey, and nesting opportunities for a variety of mammals (McElhinny et al., 2005; Nilsson and Wardle, 2005). Heterogeneous canopies offer climbing opportunities to semi-arboreal species, while a rich understory benefits rodents and other small prey mammals, which are key prey for many mammalian predators that also benefit from the shelter provided by vegetation.

Mapping understory and canopy structural features using traditional field methods is time-consuming and costly, especially at large spatial scales. Airborne laser scanning (ALS) offers an efficient approach to modeling of vegetation three-dimensional structure over extensive areas. ALS data is becoming increasingly available through national open-access schemes, enabling studies of forest structure at extensive scales.

Previous ecological studies using ALS for mammal species have typically focused on regional-scale study areas covering a few hundred km². For example, Tweedy et al. (2019) studied pacific marten resting habitat within an area of ~490 km² in California, and Wheelhouse et al. (2025) examined multispecies mustelid co-occurrence across ~350 km² in British Columbia. With the combination of ALS data and species occurrence information from, for example, citizen-science initiatives, it is now possible to investigate habitat associations across entire countries, as has been done in Denmark (42,394 km^2) where local richness of birds was studied using ALS data (Davison et al., 2023). In animal ecology, ALS has been widely used to model species richness, diversity, and habitat suitability across multiple taxa, demonstrating that forest structural features are important drivers of faunal biodiversity (Toivonen et al., 2023). Nevertheless, ALS data is underutilized for certain mammal groups, such as mustelids.

Studying mustelids is timely, as many mustelid species' populations are declining, and even those listed as Least Concern may face unrecognized threats (Lindén and Piha, 2024; Wright et al., 2022). Small

---

* Corresponding author.
E-mail address: pinja-emilia.lamsa@aalto.fi (P.-E. Lämsä).

https://doi.org/10.1016/j.foreco.2026.123742
Received 30 December 2025; Received in revised form 20 March 2026; Accepted 24 March 2026

mustelids are elusive and difficult to study (Barros et al., 2024), leaving major ecological knowledge gaps. They are key predators of small rodents (Korpela et al., 2014) forming a well-known model-system of predator–prey dynamics in boreal ecosystems, where changes in their populations can alter dynamics and potentially affect forest regeneration in unknown ways (Ylönen et al., 2019).

This study assesses the nation-wide application of airborne laser scanning data, in combination with established environmental predictors, to identify habitat characteristics relevant to three mustelid species in Finland: pine marten (*Martes martes*), stoat (*Mustela erminea*) and least weasel (*Mustela nivalis*). We demonstrate, to our knowledge for the first time, how ALS data can be used to study mustelid occurrence across an entire country, and we also discuss the usefulness of this type of remote sensing data for mapping habitats of different mustelid species.

2. Materials and methods

2.1. Study area

The study area encompasses mainland Finland (304 000 km²), represented by airborne laser scanning (ALS) data collected from 173 flight campaigns conducted between 2013 and 2022 (Table S1). The combined ALS flight campaign areas provide near-complete coverage of the country (Fig. 1). The nationwide ALS coverage enabled the examination of large-scale spatial patterns across diverse forest and land cover types.

Finland is situated mostly within the boreal forest zone, characterized by extensive coniferous forests mixed with peatlands and waterbodies. Agricultural areas are heavily concentrated in the southwestern and western parts of the country, whereas peatlands are widespread in central and northern regions.

2.2. Study species and hypotheses

We studied three common mustelid species: pine marten, stoat and least weasel. This enabled a meaningful comparison of how well ALS-based habitat measures explain variation in species occurrence.

The pine marten is a generalist predator (Zhou et al., 2011). In Fennoscandia, pine martens are typically associated with mature, spruce-dominated or mixed forests that offer dense canopy cover and structural complexity, including standing deadwood for nests (Angoh, 2024; Brainerd and Rolstad, 2002). Although frequently referred to as an old-growth forest specialist (Angoh, 2024; Twining et al., 2020), the species can also persist in various successional stages (Brainerd and Rolstad, 2002) and in human-modified landscapes (Mergey et al., 2011), provided that sufficient tree cover remains (Mergey et al., 2023). However, such areas may support lower densities and consequently affect population structure (Twining et al., 2020). Pine martens generally avoid clearcuts, young stands and open habitats (Brainerd and Rolstad, 2002), but may occasionally use edge or agricultural areas when prey availability is low (Cano-Martínez et al., 2021). While they mainly prey on small mammals, especially voles, it can switch to

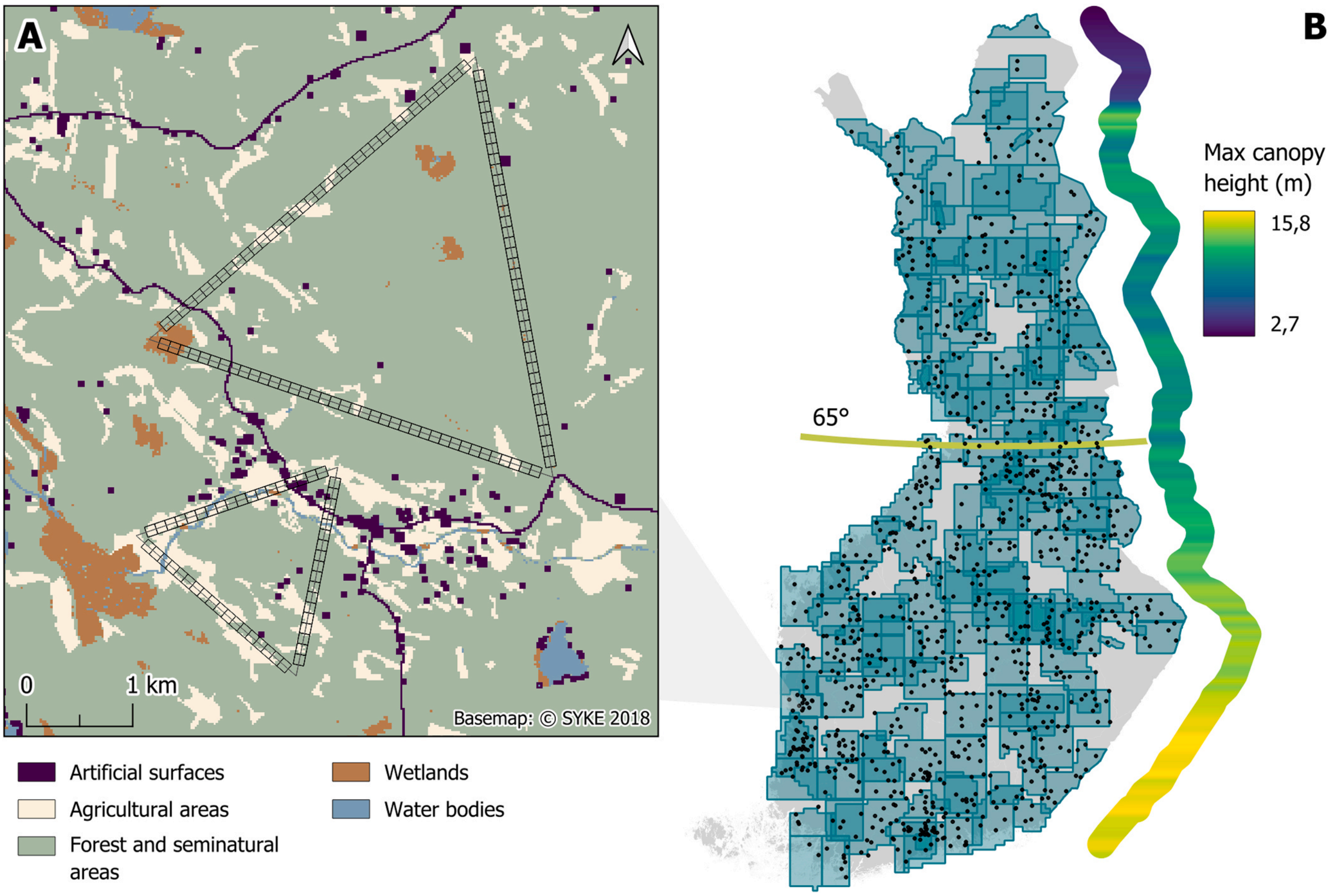

Fig. 1. Map of Finland (Panel B) illustrating the study design, including wildlife and field triangles (black dots), over the areas covered by ALS flight campaigns (blue rectangles). The green line (Panel B) indicates the 65° latitude, which was used to divide Finland into northern and southern regions for the purposes of this study. The polygon on the right (Panel B) shows the latitudinal trend of maximum canopy height across Finland. Panel A illustrates wildlife triangles (larger, 12 km census line) and field triangles (smaller, 6 km census line), which were divided into 100 m × 100 m grid cells with corners omitted. Land cover classes (Panel A) were derived from the CORINE Land Cover dataset.

alternative prey based on availability (Twining et al., 2019). The population has been increasing in northern Finland but declining in the south (Lindén and Piha, 2024). Pine martens are legally hunted in Finland and are classified as Least Concern both nationally and globally (Herrero et al., 2016).

The stoat is a smaller semi-generalist mustelid, that mainly preys on small rodents (Klemola et al., 1999). The species occurs throughout Finland, with higher densities in northern Finland. Stoats occupy a wide range of habitats following the distribution of their prey, hence, favoring edge habitats, farmlands and mosaics of open and forested terrain that support high small-mammal abundance (Cano-Martínez et al., 2021; Klemola et al., 1999; Sidorovich et al., 2008). They tend to prefer farmland and wetland habitats when voles are numerous but increasingly use woodland and forested areas during low-vole periods (Klemola et al., 1999). Stoats are generally mobile animals, but their habitat use varies with sex, vole abundance and season. Individuals tend to be more localized during winter and move more extensively in spring and summer, when juveniles may disperse several kilometers per day (Martin et al., 2011). To some extent, stoats can also access rodents in their burrows during snowy seasons (Cano-Martínez et al., 2021). Stoats are also a game species in Finland and are listed as Least Concern nationally and globally (Reid et al., 2015). However, recent population assessments indicate declines in many regions (Lindén and Piha, 2024).

The least weasel is the world's smallest carnivore and a specialist predator of voles (Ylönen et al., 2019). The species is distributed throughout Finland, with higher population densities towards the south. As a vole specialist, least weasel occurs wherever small rodents are abundant (Cano-Martínez et al., 2021; Klemola et al., 1999; Sidorovich et al., 2008), typically favoring edge habitats, meadows, and young forests that sustain high prey densities while providing dense vegetation cover from larger predators (Barros et al., 2024; Zub et al., 2008). During winter least weasels occupy subnivean space for thermoregulation and to hunt voles. Least weasels are protected under the Finnish Nature Conservation Act (NCA 2023/9) and are listed as Least Concern both nationally and globally (McDonald et al., 2019). Nonetheless, recent population estimates suggest a marked decline across the country in recent decades (Lindén and Piha, 2024).

Based on previous literature on mustelid ecology and forest structure, we formulated the following species-specific hypotheses regarding how ALS-derived structural metrics and environmental variables relate to occurrence probability.

Given its association with mature, structurally complex forests and avoidance of open habitats, we hypothesize that pine marten occurrence is positively associated with forest structural characteristics measurable with ALS, such as taller and more vertically complex canopies and higher mid- to upper-canopy density, which provide shelter, foraging opportunities, and arboreal pathways. Occurrence is expected to decrease in open or heavily human-influenced habitats.

For semi-generalist stoats we hypothesize that their occurrence shows more variable dependence on forest structure, with moderate canopy height variability or some upper-canopy structure potentially favoring stoats where it coincides with productive edges or mixed habitats. Overstory canopy density is unlikely to be a major driver. Stronger positive effects are expected from higher herbaceous-layer cover, which provides concealment and foraging opportunities, and from landscapes with higher proportions of agricultural land, mixed forests, and habitat edges that support abundant small mammals.

We hypothesize that least weasel occurrence is weakly related to ALS-derived overstory metrics and may decrease in areas with tall or dense tree canopies. Occurrence is expected to increase with higher herbaceous-layer cover, which provides concealment from avian predators and hunting routes, and with higher proportions of open or edge habitats, that support high vole densities, while decreasing in large, continuous closed-canopy forests.

2.3. Mustelid data and sampling design

We obtained pine marten, stoat and least weasel snow-track observations from the Finnish wildlife triangle and field triangle censuses (hereafter referred to as "triangles"), coordinated by the Natural Resources Institute Finland. These long-term monitoring programs provide annual data on the relative abundances and population trends of Finnish wildlife (Lindén and Piha, 2024). Wildlife triangles are permanent 12 km line transects forming an equilateral triangle with 4 km sides, established in forest-dominated landscapes. Field triangles are permanent 6 km transects (2 km per side) located in heterogeneous agricultural mosaic landscapes (Lindén et al., 1996; LUKE, 2025). Collectively, more than 2000 triangles cover both forested and agricultural regions, of which on average 1000 per year are surveyed. Our analyses were based on data collected during 2013–2022.

In winter, both triangles are surveyed by volunteers who ski the census route and record game animal snow tracks that cross the line. Wildlife triangles are typically surveyed between January 15 and February 29, with the northern regions extending the window to March 15, whereas field triangles are surveyed from January 1 through March 5. The census methods are described in detail by Helle et al. (2016).

Snow-track observations were available in two complementary formats: i) point data, giving the exact locations where observed tracks cross the census line, and ii) triangle-level records, which summarize the total number of tracks counted per triangle, explicitly including also zeros (absences). We used the point data as our primary source of data, to derive more precise presence–absence data for analysis, and used the triangle-level records to identify triangles with zero detections (absences) and to define the spatial extent of the surveyed census lines.

Each triangle census line was divided into 100 m × 100 m grid cells, with corner sections omitted to avoid overlap between cells (Fig. 1). Each cell was then assigned a binary value indicating species presence or absence. If a cell overlapped with the exact location of recorded snow tracks, it was assigned a value of 1 (presence). Otherwise, it was assigned 0 (absence). Triangles with only triangle-level track count data (lacking the point data with exact locations of the observed tracks), as well as census-line segments that were skipped and thus not surveyed, were omitted from the analysis. The workflow for selecting observations was consistent across all species.

Accumulation days — the number of days during which new snow tracks have been accumulated prior to the survey — were calculated from the last snowfall or from a preliminary snow-track survey conducted before the official census. Because snow tracks become increasingly difficult to detect over time, a threshold of maximum nine accumulation days was applied to minimize detection bias. Observations with missing information regarding the accumulation days were also excluded.

2.4. Airborne laser scanning data

2.4.1. Data acquisition

ALS data (National Land Survey of Finland, 2025a, 2025b) were obtained from the National Land Survey of Finland in March 2025, under the CC BY 4.0 License (https://creativecommons.org/licenses/by/4.0/). We used data from 2013 to 2022, collected during the leaf-on period, with acquisition windows adjusted for latitudinal differences in growing season length. The onset of the growing season occurs later in northern Finland, therefore, based on long-term statistics from the Finnish Meteorological Institute statistics (Finnish Meteorological Institute, 2026), in southern Finland (south of 65°N), data were acquired between June 1 and August 31, whereas in northern Finland (north of 65°N), data were acquired between June 15 and August 31.

Selected flight campaigns are listed in Table S1. Flight altitudes ranged between 855 m and 3050 m above ground level. Several scanner models were used (Table S1) all operating at the wavelength of 1064 nm and capable of recording 4 or more returns per pulse, depending on the scanner model. The ALS data had been preprocessed by the National Land Survey of Finland, including removal or labeling of returns at overlap areas between flight lines as well as erroneous returns in the sky or below ground. We removed all overlap and erroneous returns before further processing.

The pulse densities for data acquired prior to 2020 varied between 0.5 and 2.65 pulses m^{-2}. The data acquired since 2020 had been automatically decimated by the data provider to a density of 0.5 pulses m^{-2}. Such pulse densities are typical of national-scale ALS acquisitions and are generally sufficient for deriving canopy height and other area-based forest structure metrics (Gobakken and Næsset, 2008), although vegetation close to the ground may be less accurately represented due to fewer returns penetrating the canopy. The limitation is largely caused by signal occlusion, where upper canopy elements intercept incoming laser pulses and reduce the number of returns from lower vegetation strata, particularly in dense forests (Crespo-Peremarch et al., 2020). Despite the variation in pulse density among our dataset, the relatively large size of our sampling units (100 m × 100 m) ensures that each cell still contains a substantial number of laser returns, so that the derived area-based structural metrics are expected to remain robust.

2.4.2. ALS-derived vegetation structure metrics

We calculated rasters of vegetation structure metrics (16 m × 16 m cell size) for each laser scanning flight campaign area. These included measures of canopy height distribution, cover, vertical density, and structural diversity (Table 1). Each metric captures complementary aspects of forest structural features that may influence mustelid habitat use, as suggested by the literature (see Section 2.2). A 16 m × 16 m resolution was chosen because it corresponds to the national standard for forest inventories in Finland.

The ALS data were processed using a workflow that combines LAStools (LAStools, 2025), GDAL (Rouault et al., 2025) and in-house C+ + modules. First, ALS returns were classified as ground and non-ground returns, using tool “lasground”. Second, the point-clouds were normalized, i.e., each return’s height above ground was calculated, using tool “lasheight”, which computes each return’s height above the ground surface defined by a triangulated irregular network constructed from the ground returns. Returns below the estimated ground surface were assigned a height value of zero. Vegetation structure metrics (Table 1) were then calculated from the normalized point cloud, using our C+ + code.

2.5. Other environmental data

Daily average temperature and average snow depth data (Table 2) were extracted from 10 km resolution national geospatial grids provided by the Finnish Meteorological Institute (FMI). The datasets covered the years 2013–2022 and provided spatially continuous weather information across Finland. The data is described in detail by Aalto et al. (2016). Temperature was included as a variable as it is known to affect detection probability of pine martens (Angoh, 2024), and it could have similar effects on stoat and least weasel. Similarly, snow depth is known to influence hunting efficiency, movement patterns, and habitat use among mustelids (Angoh, 2024; Cano-Martínez et al., 2021; Willebrand et al., 2017), ultimately affecting the number of snow tracks observed.

Land cover data (Table 2) were obtained from the Finnish CORINE Land Cover 2018 dataset (EU Copernicus Land Monitoring Programme), which provides 20 m × 20 m resolution national land cover and land use classifications. This data provides description of habitat composition and landscape configuration, which helps to distinguish between major habitat types that influence prey availability and general habitat use by mustelids (see Section 2.2).

We also derived distance-based metrics describing habitat configuration (Table 2): mean distances to artificial and agricultural surfaces, and mean distance to forest edges. These factors are associated with the occurrence patterns of the study species, though their effects differ (see

Table 1
ALS-derived vegetation structure metrics used to describe canopy height, cover, and vertical structure. Metrics were calculated using all ALS returns (i.e., single, first-of-many, last-of-many, and intermediate) to maximize the number of returns and thus detail in vertical characterization of the canopy. The only exception were canopy cover metrics, which were calculated using returns categorized as first-of-many or single in a pulse, as these have been found to produce reliable estimates of canopy cover without empirical calibration (Korhonen et al. 2011). In all calculations, returns having a height value larger than 1.3 m were classified as tree canopy returns. h_i= height from ground for ALS return i [m]; $h_{rel,i}$ = relative height between the bottom of canopy (1.3 m) and maximum height for ALS return i [%]; n = number of ALS returns analyzed; p = chosen percentile in the height distribution (e.g. 10th, 50th, 95th percentile); p_i= percentile of i-th return; f_i = fraction of returns within the i-th height interval.

Variable	Description	Equation	Unit
Metrics describing tree canopy height, calculated using all returns belonging to tree canopy ($h_i > 1.3$ m)			
Height percentiles (10th, 20th, 30th, 40th, 50th, 60th, 70th, 80th, 90th, 95th, 99th)	Returns are ordered from lowest to highest, and the height values corresponding to the selected percentiles are calculated using linear interpolation.	$P(p) = h_i + \frac{p - p_i}{p_{i+1} - p_i}(h_{i+1} - h_i)$	Meters (m)
Mean height of tree canopy	Mean height of canopy returns.	$\overline{h} = \frac{1}{n}\sum_{i=1}^{n} h_i$	Meters (m)
Metrics describing tree canopy vertical structure, calculated using all returns belonging to tree canopy ($h_i > 1.3$ m)			
Relative density of returns in a given canopy layer	Number of returns at height bins (0–10%, 10–20%, 20–30%, …, 90–100%, where 0% = 1.3 m and 100% = max. h) divided by all tree canopy returns.	$D(h_{rel,low} - h_{rel,upp}) = \frac{n(h_{rel,low} < h_{rel,i} \leq h_{rel,upp})}{n} \times 100$	Percentage (%)
Standard deviation of vegetation height	Standard deviation of return heights calculated using the estimator for sample standard deviation.	$\mathrm{SD}(h) = \sqrt{\frac{\sum_{i=1}^{n}(h_i - \overline{h})^2}{n-1}}$	Meters (m)
Coefficient of variation of vegetation height	The standard deviation of return heights is divided by the mean height. Produces a normalized measure of height variability.	$\mathrm{CV}(h) = \frac{\mathrm{SD}(h)}{\overline{h}} \times 100$	Percentage (%)
Skewness of vegetation height	Skewness of return heights calculated using adjusted Fisher–Pearson standardized moment coefficient.	$\mathrm{Skewness}(h) = \frac{n\sum_{i=1}^{n}\left(\frac{h_i - \overline{h}}{SD(h)}\right)^3}{(n-1)(n-2)}$	Meters (m)

(continued on next page)

Table 1 (*continued*)

Variable	Description	Equation	Unit
Kurtosis of vegetation height	Kurtosis of return heights calculated using adjusted Fisher–Pearson standardized moment coefficient.	$\mathrm{Kurtosis}(h) = \frac{n(n+1)\sum_{i=1}^{n}\left(\frac{h_i-\bar{h}}{SD(x)}\right)^4}{(n-1)(n-2)(n-3)} - \frac{3(n-1)^2}{(n-2)(n-3)}$	-
Shannon index	Returns are divided into vertical height bins of 0.5 m. The fraction of returns in each bin reflects tree canopy density at different heights and is used to compute structural diversity using the Shannon index.	$H = -\sum_{i=1}^{m} f_i \ln(f_i)$	-
Metrics describing canopy cover, calculated using returns categorized as single or first-of-many in a pulse			
Canopy cover of herbaceous layer	Number of returns between 0.2 m and 0.5 m divided by number of returns that are below 0.5 m	$CC_{\mathrm{herbaceous}} = \frac{n(0.2 < h_i \leq 0.5)}{n(h_i \leq 0.5)}$	Percentage (%)
Canopy cover of shrub layer	Number of returns between 0.5 m and 1.3 m divided by number of returns that are below 1.3 m	$CC_{\mathrm{shrub}} = \frac{n(0.5 < h_i \leq 1.3)}{n(h_i \leq 1.3)}$	Percentage (%)
Canopy cover of small trees	Number of returns between 1.3 m and 5 m divided by number of returns that are below 5 m	$CC_{\mathrm{small\ trees}} = \frac{n(1.3 < h_i \leq 5)}{n(h_i \leq 5)}$	Percentage (%)
Canopy cover of tree layer	Number of returns above 1.3 m divided by total number of returns	$CC_{\mathrm{tree\ layer}} = \frac{n(h_i > 1.3)}{n}$	Percentage (%)

Section 2.2).

Table 2
Other environmental variables used to describe weather conditions, land cover and landscape composition.

Variable	Description	Unit	Data source	Spatial resolution of source data
Distance to forest edge	Mean distance to the nearest forest edge pixel.	m	ALS + CORINE	16 m × 16 m and 20 m × 20 m
Snow Depth	Snow depth at 8 am, 10 km × 10 km gridded observations	m	FMI	10 km × 10 km
Temperature	Daily mean temperature, 10 km × 10 km gridded observations	°C	FMI	10 km × 10 km
Percentage of artificial surfaces	The relative proportion of pixels belonging to Corine classes 1–16.	%	CORINE	20 m × 20 m
Percentage of arable land, pastures, crops	The relative proportion of pixels belonging to Corine classes 17–22.	%	CORINE	20 m × 20 m
Percentage of broadleaf forest	The relative proportion of pixels belonging to Corine classes 23–24.	%	CORINE	20 m × 20 m
Percentage of coniferous forest	The relative proportion of pixels belonging to Corine classes 25–27	%	CORINE	20 m × 20 m
Percentage of mixed forest	The relative proportion of pixels belonging to Corine classes 28–30.	%	CORINE	20 m × 20 m
Percentage of sparse forest	The relative proportion of pixels belonging to Corine classes 33–37.	%	CORINE	20 m × 20 m
Percentage of inland or coastal waterbodies	The relative proportion of pixels belonging to Corine classes 47–49.	%	CORINE	20 m × 20 m
Distance to artificial surface	The Euclidean distance from a point within the study area to the nearest pixel classified as artificial surface (e.g. urban fabric, artificial areas, construction sites, transport units).	m	CORINE	20 m × 20 m
Distance to agricultural areas	The Euclidean distance from a point within the study area to the nearest pixel classified as agricultural areas (e.g. arable land and pastures)	m	CORINE	20 m × 20 m

2.6. Data aggregation

ALS flight campaign metadata were spatially joined to the centroid of each grid cell (100 m × 100 m) to identify overlapping flight campaigns. Where multiple ALS campaigns covered a given cell, the campaign closest in time to the mustelid survey was selected to ensure temporal consistency between structural and occurrence data. Observations were included if the year of the triangle survey fell within ±2 years of the corresponding ALS data, regardless of canopy height. If the ALS data were acquired after the field survey, observations were also accepted up to five years apart, provided that the minimum canopy height within the cell was at least 5 m. The minimum canopy height was derived from the 95th percentile of all canopy returns, which has been shown to predict dominant tree height accurately (Kotivuori et al., 2016). Grid cells with scan angles $> 20^\circ$ were excluded, totaling 441 cells from 20 flight campaigns, as larger scan angles may bias canopy metrics (Dayal et al., 2020).

A vegetation mask was created to restrict analyses to vegetated terrain. The mask was derived from the combination of the ALS point density raster and CORINE land cover data. Agricultural areas (class 2), forests and seminatural areas (class 3), and wetlands (class 4) were included, except for "non-irrigated arable land" (class 2.1.1) to exclude open croplands. Cells were classified as vegetated where ALS pulse density exceeded 0.2 pulses m^{-2} and CORINE indicated forest or vegetation cover. This vegetation mask was applied to all ALS-derived metrics to ensure analyses reflected structural variation within vegetated habitats only.

For each grid cell (100 m × 100 m), we extracted mean values of all ALS-derived vegetation metrics (Table 1) using a zonal statistics approach implemented in Python (geopandas (Jordahl et al., 2020), rasterio (Gillies, 2018), rasterstats (Perry, 2017)). Mean temperature and snow depth were calculated as the averages of the census day and two preceding days to reflect short-term conditions during track detection. The fraction of area covered by different land-cover types was derived from CORINE (Table 2). Distances to urban areas and agricultural land were computed from Euclidean distance rasters at 20 m resolution, generated from binary masks of each land-cover type (Table 2).

Forest edges were identified as boundaries between forested and non-forested cells. Cells with canopy cover larger than 10% and 95th percentile of canopy return heights larger than 5 m were classified as forests. These criteria were applied to ALS-derived canopy metrics at 16 m resolution, using a binary forest/non-forest mask derived from the 20 m CORINE land cover raster for Finland, where vegetated land-cover classes were coded as 1 and all other classes as 0. Distance to forest edge was calculated as the mean Euclidean distance from forested cells to the nearest edge. Distance to forest edge for each grid cell was then calculated as the mean of these distances across all 16 m × 16 m raster cells intersecting a 100 m × 100 m cell. Cells with missing or no-data values were excluded.

The final mustelid dataset included 1068 triangles from which 947 were wildlife triangles and 121 field triangles. Across these, the pine marten, stoat and least weasel had 337854, 341035 and 342920 100 m × 100 m sampling units, respectively. Pine marten was detected 4087 times (1.2% of cells), stoat 1826 times (0.5% of cells) and least weasel 1351 times (0.4% of cells).

2.7. *Statistical analysis*

Prior to modelling, data exploration was conducted to detect potential outliers, assess independence of observations, and evaluate collinearity among predictors, following the protocol presented in (Zuur et al., 2010). Potential outliers were screened visually using boxplots and Cleveland dotplots to identify any extreme values. No observations were identified as markedly inconsistent with the remainder of the dataset, and therefore no data points were removed on the basis of outlier diagnostics. To assess multicollinearity, Variance Inflation Factors (VIF) were calculated using the “car” package (Fox and Weisberg, 2019). Three ecologically relevant covariates were preselected and retained in the analysis regardless of their VIF values (canopy cover of the tree layer, 95th percentile of canopy return heights, and canopy cover of the herbaceous layer). Canopy cover of the tree layer and the 95th percentile of canopy return heights were included because they capture complementary aspects of forest vertical and horizontal complexity. Canopy cover reflects horizontal foliage density and shapes light availability and understory composition (Majasalmi and Rautiainen, 2020), and, in turn, the distribution of small mammal prey such as voles and other rodents (Savola et al., 2013; Wegge and Rolstad, 2018). The 95th percentile of canopy return heights is widely used as a proxy for dominant canopy height. It is not strongly affected by understory vegetation or ground returns, thus, providing accurate representation of the upper canopy (Kane et al., 2010). Canopy cover of the herbaceous layer was additionally retained as it quantifies ground-level vegetation (McElhinny et al., 2005), providing shelter and movement corridors for small mammals, including both prey and mustelid predators. The Pearson’s correlation coefficients between the explanatory variables were checked (requirement: $|r| < 0.7$) to avoid strong correlations. Among the remaining variables, those with the highest VIF were iteratively removed until all VIF values were under a threshold ($\mathrm{VIF} < 3$). This ensured that collinearity among explanatory variables did not bias model estimation.

We modelled species presence using spatial hierarchical generalized linear mixed-effects models implemented with the package sdmTMB (Anderson et al., 2022). Models were fitted with maximum marginal likelihood estimation. We used a binomial error distribution with a logit link function to model the binary response variable (presence = 1, absence = 0). A random intercept for “triangle ID” was included to account for repeated observations within censuses.

Spatial and temporal dependencies were modelled jointly using a spatiotemporal random field, parameterized with a Matérn covariance structure for spatial correlation and a first-order autoregressive (AR1) process to capture temporal correlation among years. As an inherent property of the modelling principles of spatial dependence in sdmTMB, a triangulated mesh was constructed from the centroid coordinates of census cells using k-means clustering. The mesh defines the spatial domain over which the Matérn field is estimated and enables computationally efficient approximation of spatial covariance.

The fixed effects included covariates describing climate (mean temperature, snow depth), land cover composition (proportion of urban, agricultural, broadleaved forest, mixed forest, sparse forest, and water areas), forest structure (relative canopy density at mid and upper height layers, 95th percentile of canopy heights, canopy height variability and kurtosis, and canopy cover of the herbaceous and tree layers), and landscape configuration (distance to forest edge, artificial surfaces and agricultural areas). In total, we included 7 ALS metrics and 11 other environmental metrics in the models. Continuous covariates were standardized to zero mean and unit variance. Sampling effort (log-transformed number of accumulation days) was included as a covariate in all models to account for variation in observation effort.

Model assumptions were verified by plotting residuals against fitted values and against each covariate in the model. Standardized residuals were simulated using the “DHARMa” package (Hartig et al., 2022) to compute simulation-based randomized quantile residuals, which are standardized residuals expected to follow an approximately Uniform(0, 1) distribution and to be independent of fitted values and covariates if the model is correctly specified. We tested for over- or underdispersion, and zero-inflation was also examined by comparing observed and simulated frequencies of zeros. The presence of spatial autocorrelation in the residuals was assessed by calculating Moran’s I with the “spdep” package (Bivand et al., 2022). All model fitting, diagnostics and visualization were performed using R (version 4.4.0; R Core Team, 2024).

3. Results

3.1. *Effects of covariates on species presence*

The results demonstrate that ALS metrics describing vertical canopy structure and canopy cover, alongside landscape and climatic variables, influenced occurrence probabilities of the three species (Table 3, Table 4, Table 5). Metrics related to canopy height variability (e.g. coefficient of variation of height), canopy cover of the tree layer, and relative canopy density at mid (20–30%) and upper (40–50%) height layers emerged as important structural predictors for one or more species, although their effects differed in strength and direction among species (Fig. 2).

For the pine marten, several ALS-derived metrics and environmental variables were associated with occurrence (Table 3, Fig. 2). The

Table 3
Standardized coefficients of the logit-link binomial mixed model for pine marten.

Variable	Estimate	SE
Intercept	-5.100	0.061
95th height percentile	0.083	0.029
Relative density of canopy returns at 20–30% height	0.067	0.025
Relative density of canopy returns at 40–50% height	0.008	0.027
Coefficient of variation of vegetation height	0.071	0.026
Kurtosis of vegetation height	0.037	0.020
Canopy cover of herbaceous layer	0.028	0.022
Canopy cover of tree layer	0.194	0.032
Temperature	-0.014	0.025
Snow depth	0.111	0.038
Distance to artificial surfaces	0.180	0.027
Distance to agricultural areas	0.048	0.040
Distance to forest edge	-0.052	0.032
Percentage of artificial surfaces	-0.206	0.042
Percentage of arable land, pastures, crops	-0.209	0.039
Percentage of broadleaf forest	-0.038	0.020
Percentage of mixed forest	-0.025	0.019
Percentage of sparse forest	0.021	0.022
Percentage of waterbodies	-0.065	0.030
Effort (log Accumulation days)	0.040	0.050

Table 4
Standardized coefficients of the logit-link binomial mixed model for stoat.

Variable	Estimate	SE
Intercept	-6.170	0.090
95th height percentile	-0.007	0.044
Relative density of canopy returns at 20–30% height	0.026	0.035
Relative density of canopy returns at 40–50% height	0.093	0.036
Coefficient of variation of vegetation height	0.144	0.035
Kurtosis of vegetation height	0.054	0.029
Canopy cover of herbaceous layer	0.119	0.029
Canopy cover of tree layer	0.003	0.046
Temperature	-0.116	0.038
Snow depth	0.136	0.060
Distance to artificial surfaces	0.062	0.042
Distance to agricultural areas	-0.074	0.058
Distance to forest edge	-0.038	0.044
Percentage of artificial surfaces	0.019	0.035
Percentage of arable land, pastures, crops	0.136	0.031
Percentage of broadleaf forest	0.024	0.026
Percentage of mixed forest	0.072	0.027
Percentage of sparse forest	0.074	0.030
Percentage of waterbodies	0.041	0.034
Effort (log Accumulation days)	0.016	0.072

Table 5
Standardized coefficients of the logit-link binomial mixed model for least weasel.

Variable	Estimate	SE
Intercept	-6.730	0.102
95th height percentile	-0.009	0.045
Relative density of canopy returns at 20–30% height	-0.005	0.039
Relative density of canopy returns at 40–50% height	-0.038	0.038
Coefficient of variation of vegetation height	0.035	0.035
Kurtosis of vegetation height	0.023	0.030
Canopy cover of herbaceous layer	0.083	0.036
Canopy cover of tree layer	-0.055	0.051
Temperature	-0.225	0.045
Snow depth	-0.289	0.062
Distance to artificial surfaces	-0.062	0.056
Distance to agricultural areas	-0.057	0.073
Distance to forest edge	-0.039	0.052
Percentage of artificial surfaces	-0.002	0.037
Percentage of arable land. pastures. crops	0.039	0.033
Percentage of broadleaf forest	-0.065	0.034
Percentage of mixed forest	0.040	0.033
Percentage of sparse forest	0.016	0.035
Percentage of waterbodies	-0.019	0.041
Effort (log Accumulation days)	0.019	0.090

occurrence probability increased with higher relative canopy density at mid-canopy height (20–30%), greater canopy height variability, higher 95th percentile of canopy heights, and increased canopy cover of the tree layer. Among other environmental factors, the probability of detecting pine marten tracks increased with deeper snow depth and greater distance from artificial surfaces. Occurrence probability decreased with higher proportion of agricultural or artificial land cover or high proportion of waterbodies.

The stoat model highlighted slightly different structural associations (Table 4, Fig. 2). Occurrence probability had positive relationships with variability in canopy height, relative canopy density at upper canopy height (40–50%), and canopy cover of the herbaceous layer. Unlike the pine marten, stoats were positively associated with high proportion of agricultural, sparse and mixed forest areas. Increasing temperature decreased the occurrence (or detection) probability, whereas increasing snow depth was positively related to the probability of observing stoat tracks.

For the least weasel, fewer predictors were significant, and ALS-derived canopy metrics contributed less than for the other species (Table 5, Fig. 2). The probability of occurrence (or detection) of least weasel tracks was higher with greater canopy cover in the herbaceous layer, whereas increasing temperature, snow depth and proportion of broadleaved trees decreased the probability.

3.2. Model validation

Model validation indicated no major violations of model assumptions for any of the three species. DHARMa simulation-based randomized quantile residuals were approximately uniformly distributed and showed no systematic patterns (Figure S1, Figure S2. Figure S3). Observed and simulated zero frequencies were nearly identical, confirming that zero-inflation was not a concern. Dispersion tests utilizing DHARMa residuals (testing the null hypothesis of no over- or under-dispersion) showed dispersion parameters of 1.01 ($p = 0.548$) for pine marten, 1.04 for stoat ($p = 0.188$), and 1.08 ($p = 0.008$) for least weasel, all close to the expected value of 1. For least weasel, the test indicated mild overdispersion, but the effect size was small and other diagnostics did not reveal systematic lack of fit. We therefore considered the model adequate for inference. Inclusion of a spatio-temporal AR1 component improved model performance for pine marten ($\rho = 0.33$), indicating moderate year-to-year persistence at the national scale. For stoat ($\rho = 0.14$) and least weasel ($\rho = -0.06$), the estimated AR1 correlations were weaker. Both species have rapid and locally asynchronous population cycles. This 2–3-year periodicity could produce little or even negative lag-1 correlation, which does not contradict the presence of local temporal dynamics. Moran's I estimations suggested that model had adequately captured the spatial structure and that there was no significant spatial autocorrelation (pine marten: Moran's $I = -2.605$, $p = 0.564$; stoat: Moran's $I = -4.442$, $p = 0.611$; least weasel: Moran's $I = -4.676$, $p = 0.617$). All models included random intercepts for triangle ID. The estimated variances were 0.57 for pine marten, 0.89 for stoat, and 1.41 for least weasel, reflecting variation in species' occurrences that were not accounted for by the fixed effects. Overall, the model validation indicated that the fitted GLMMs captured the main sources of variation in the data and provided a reasonable representation of species-habitat relationships.

4. Discussion

4.1. Ecological implications of the modeling results for mustelid habitat use

This study combined ALS-derived forest structure metrics with presence–absence data of three mustelid species to examine the potential of ALS data for identifying habitat characteristics relevant to each species occurrence. Our results show that ALS-derived metrics can describe habitat structural features relevant to mustelids. The strength of responses varied from strong responses to canopy complexity in pine martens to weaker more open-habitat related associations in least weasels.

Based on our results, the pine marten is most likely to inhabit forests with dense canopy cover, variability in canopy height, and higher maximum canopy heights, indicating complex and layered forest structure. These forests provide dense and diverse habitats, and the preference corroborates with earlier studies (Brainerd and Rolstad, 2002; Twining et al., 2020). These findings are consistent with our *a priori* hypothesis that pine marten occurrence would be positively associated with taller, more vertically complex canopies and higher mid- to upper-canopy density. In terms of landscape composition, the habitats preferred by pine martens are located away from agricultural or artificial land covers or extensive waterbodies. This coincides with earlier studies (Twining et al., 2020) and suggests a preference for undisturbed and natural environments. Large waterbodies reduce the extent and connectivity of forested habitat and are typically surrounded by more open shorelines, resulting in landscapes with less continuous canopy cover and therefore less favorable conditions for pine martens. Detected pine marten occurrence increased with snow depth but was unaffected

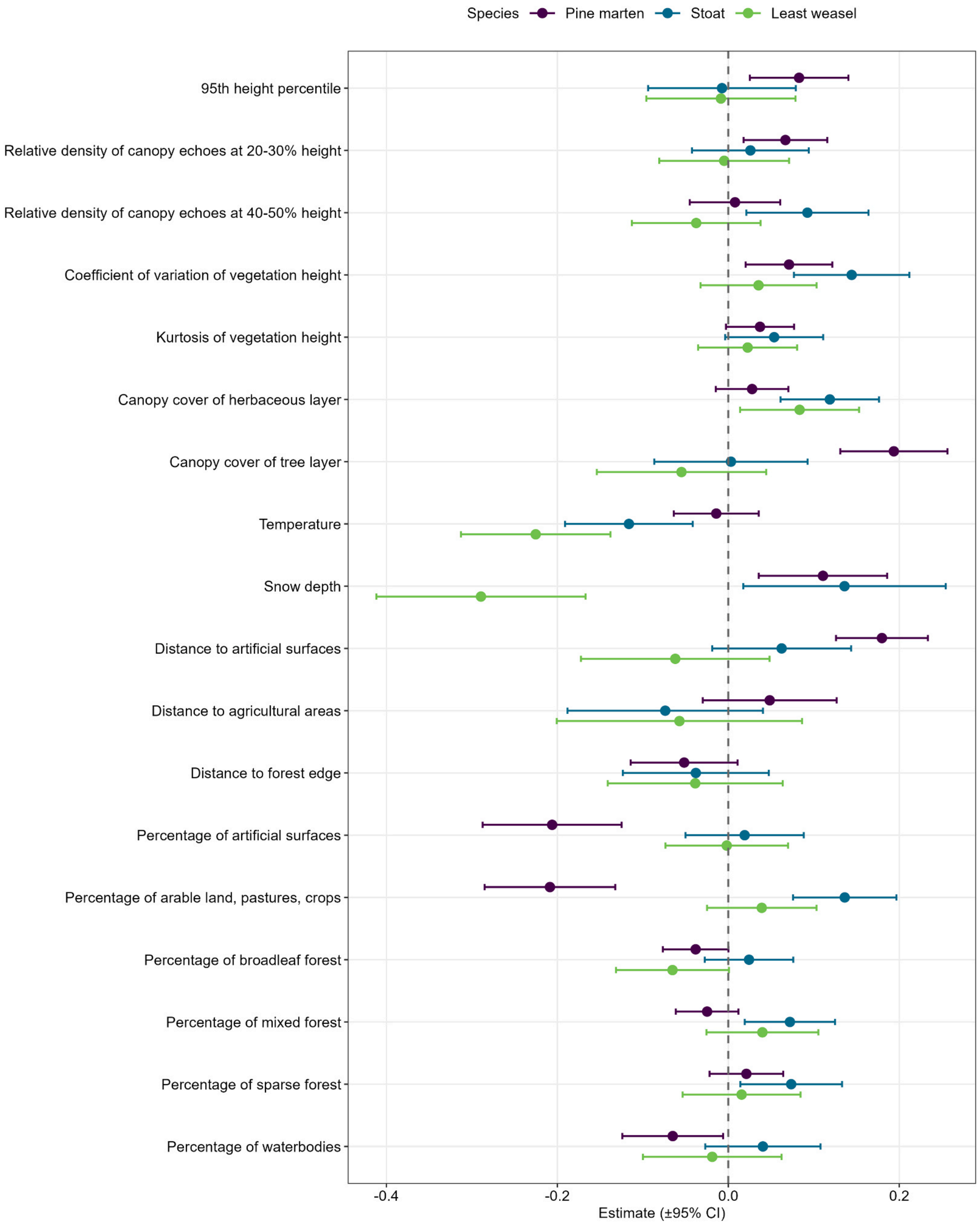

Fig. 2. Estimated standardized coefficients (β ± 95% confidence interval, CI) illustrating effect of each standardized covariate.

by temperature. Similar findings have been reported previously, suggesting that deep snow may provide favorable hunting and movement conditions and help reduce intraguild competition, particularly when rodent prey are abundant (Angoh, 2024; Cano-Martínez et al., 2021). When interpreting results for pine martens, it is important to consider that detection probability may vary among habitat types. In more open habitats pine martens are likely to move more frequently on the ground rather than using arboreal pathways, which may increase the likelihood of detecting their tracks. This could lead to an over-representation of pine marten occurrences in open habitats relative to closed forests, even if the species prefers forested environments. Overall, based on our results, the habitat preferred by pine marten is a structurally diverse forest with minimal human disturbance and sufficient snow cover, in line with our hypotheses.

On the other hand, based on our results, stoats are likely to inhabit heterogenous forests that are characterized by variation in canopy height and dense canopy coverage at higher levels. These forests feature developed overstory structures and complexity at lower levels, as indicated by the importance of canopy cover within the herbaceous layer. This partly supports our hypothesis of a weaker but still positive association with forest structural heterogeneity, combined with a stronger role of herbaceous-layer cover. Unlike the pine marten, stoats show a positive association with mixed forests areas, sparse forest regions, and agricultural landscapes. This indicates utilization of more diverse and open environments, which has been recognized in prior studies as well (Klemola et al., 1999; Sidorovich et al., 2008), and is in line with our expectation that stoats would benefit from mosaics of agricultural and forested habitats that support high small-mammal abundance. Stoat activity also increased with snow depth but, unexpectedly, declined with increasing temperature. Stoats tend to utilize the subnivean space under the snow during cold periods to conserve heat, and hunt voles. The positive response to snow depth could, similarly to the pine marten, reflect their ability to exploit subnivean space for hunting and to benefit from the shelter and insulation provided by snow cover. Higher temperatures, on the other hand, may reduce stoat activity, as their greater energy requirements in cold conditions, likely promote more movement at lower temperatures. Overall, the results suggest that stoats use heterogeneous forests characterized by a developed overstory and a well-developed herbaceous layer, within landscapes that include both forested and agricultural areas, broadly supporting our initial hypotheses.

The least weasel exhibited weaker relationships with ALS metrics, suggesting broader habitat tolerance and possibly a stronger dependence on prey abundance or climatic conditions than strictly on vegetation structure. This agrees with our hypothesis that least weasel occurrence would be largely independent of overstorey metrics and only weakly linked to forest canopy structure, although at least some modest effects of mid-canopy cover or landscape composition had been expected due to their potential to provide shelter from avian predators and other larger carnivores. Occurrence was higher in areas with greater herbaceous-layer cover but declined with increasing temperature, snow depth and broadleaf proportion. For a vole-specialist like the least weasel (Ylönen et al., 2019), prey availability might have a more important role in habitat selection than canopy structure. The least weasel also utilizes more ground-level structures to hide from other predators, such as pine marten, which especially favors mid-level canopy cover based on our results. Another favorable aspect of the herbaceous layer is its vole density, as most of them live in that layer providing steady selection of prey items (Ecke et al., 2002). The positive association with herbaceous-layer cover thus matches our prediction that herbaceous vegetation would be particularly important for this species. However, most other structural and land-cover variables showed very weak or non-significant associations, indicating that many of the potential cover-related benefits from mid- or upper-canopy structure were not detectable at the scale of our analysis. The least weasel also had an unexpected decrease in activity with increasing temperature. Similarly to stoat, lower temperatures increase energy demand (Ylönen et al., 2019), which likely leads to more movement. Thus, increased temperature might lower least weasel activity. When optimal, least weasels hunt and seek shelter in the subnivean space during winter, which also could affect their detection probability. Nevertheless, consistent with this behavior, occurrence probability in our study also declined with increasing snow depth. Avoidance could reflect the energetic costs and physical limitations associated with moving and hunting under very deep or crusted snow, as well as reduced prey accessibility (Cano-Martínez et al., 2021). Overall, results suggest use of relatively open, coniferous or mixed forests providing ground cover, while highlighting that environmental and climatic constraints, or prey availability, may be more influential than canopy structure in shaping least weasel distributions, as hypothesized.

4.2. *ALS data as a tool for large-scale mustelid habitat assessment*

This study highlights both the potential and limitations of using ALS-derived forest structure metrics for large-scale occurrence modeling of small and medium-sized mustelids. Occurrence and habitat selection models often face a trade-off between homogenization at large spatial scales and non-transferability at small spatial scales (Paton and Matthiopoulos, 2016). Studies conducted in restricted regions can capture detailed habitat relationships but may fail to generalize because they reflect the local habitat composition and conditions of a specific area. This becomes especially problematic for species inhabiting heterogenous landscapes, such as Finland's mosaic of boreal forests. On the contrary, large-scale models allow estimation of more robust and generalizable habitat associations (Paton and Matthiopoulos, 2016). Nationwide modeling therefore provides essential insights into the species' responses across heterogenous landscapes and could detect consistent patterns that regional studies may overlook. For mustelids, whose ecology has mostly been studied at local scales, the national ALS datasets offer an opportunity to derive nationwide habitat associations relevant for conservation, monitoring and forecasting.

ALS metrics describing vertical canopy structure and canopy cover contributed substantially to the occurrence predictions for pine marten and stoat. In contrast, ALS metrics were less informative for least weasel, whose occurrence was primarily associated with herbaceous-layer cover. This species could be strongly linked to microhabitat conditions and prey availability, aspects that ALS cannot fully capture. Moreover, the selected ALS metrics may not fully capture ground-level structural complexity relevant to least weasel ecology. This reflects a general limitation of ALS datasets, as near-ground vegetation is difficult to sample due to occlusion by overstorey layers and inaccuracies in separating ground and low vegetation returns. These constraints are particularly present in typical national-scale acquisitions with relatively low pulse densities, where fewer laser pulses penetrate to lower vegetation strata. Vegetation at 0.2–0.5 m height approaches the lower limits of ALS detection accuracy (White et al., 2016) and without validation data, the potential impact of measurement error remains uncertain. Nonetheless, the detected correlation with herbaceous-layer cover suggests that even coarse ALS-derived ground-level metrics contain ecologically meaningful information. Future occurrence modeling for least weasel may benefit from integrating full-waveform ALS (Hancock et al., 2017), which may provide more detailed three-dimensional representation of near-ground vegetation. Although pulse density does not strongly affect typical ALS metrics used for describing tree canopy (Gobakken and Næsset, 2008), higher pulse density can increase the chance that enough pulses reach the ground vegetation.

Also, the chosen modelling approach may influence the ecological findings. Here we used spatial hierarchical GLMMs with a Matérn covariance structure, AR1 temporal process, and random intercept for repeated censuses, providing interpretable estimates of how ALS-derived forest structure and other environmental predictors relate to mustelid occurrence across Finland. Alternative approaches, such as machine-learning methods (e.g. Random Forests, Davison et al., 2023), could complement this framework by capturing more complex nonlinear relationships and interactions among predictors, although having a higher risk of overfitting. While we expect the main ecological patterns here to be robust across reasonable modelling choices, future work comparing different model structures could help to evaluate the robustness of the observed relationships and refine habitat suitability predictions for these species.

Overall, ALS enables the identification of structural habitat features relevant for pine marten and stoat across an entire country but appears insufficient on its own for species with highly specialized, low-level habitat use such as the least weasel. Future work on modeling occurrence or habitat suitability of mustelids should integrate ALS data with field-based prey surveys, fine-scale snow metrics, and interspecific interaction data to better capture their ecological requirements and behavioral constraints. However, obtaining simultaneous high-quality and high spatial resolution ground reference data for all these components remains a significant challenge.

5. Conclusions

We showed how ALS-derived forest structure metrics, combined with environmental covariates, can predict occurrence among three mustelid species, for the first time at a national scale. These findings reveal distinct habitat preferences among pine marten, stoat and least weasel, emphasizing the significance of canopy structure. These results indicate that the structural complexity of forests could promote biodiversity and aid conservation efforts by benefiting mustelids. ALS metrics are powerful tools for predicting occurrence patterns in monitoring data, offering detailed insight into structural features across large areas and enhancing traditional methods that are impractical at broader scales.

CRediT authorship contribution statement

Pinja-Emilia Lämsä: Writing – original draft, Visualization, Software, Methodology, Investigation, Formal analysis, Data curation, Conceptualization. **Aarne Hovi:** Writing – review & editing, Software, Methodology, Data curation, Conceptualization. **Andreas Lindén:** Writing – review & editing, Methodology, Data curation, Conceptualization. **Miina Rautiainen:** Writing – review & editing, Supervision, Methodology, Conceptualization.

Declaration of Competing Interest

The authors declare that they have no known competing financial interests or personal relationships that could have appeared to influence the work reported in this paper.

Acknowledgements

We thank the KAUTE Foundation for supporting Lämsä's research and the Research Council of Finland (grants 374133 and 363934) for funding Rautiainen and Hovi. We thank Markus Melin for insightful discussions regarding the study design. We also thank all volunteers who contributed to the collection of wildlife and field triangle data in Finland. We acknowledge CSC – IT Center for Science, Finland, for computational resources.

Appendix A. Supporting information

Supplementary data associated with this article can be found in the online version at doi:10.1016/j.foreco.2026.123742.

Data availability

The mustelid data is owned by Natural Resources Institute Finland (LUKE) and is available only with permission from the data owner. ALS data were obtained from the National Land Survey of Finland; land cover data from the CORINE Land Cover 2018 dataset via the Finnish Environment Institute (SYKE) open data portal (https://ckan.ymparisto.fi/dataset/corine-maanpeite-2018); and meteorological data from the Finnish Meteorological Institute's (FMI) "Gridded daily meteorological data in Finland (1981–2020)" (https://etsin.fairdata.fi/dataset/55809c24-475d-4928-8161-3f67791c3ab0, https://etsin.fairdata.fi/dataset/c63d696a-8d42-44aa-8508-9024ee05cfa7); these are available under a CC BY 4.0 license.

References

Aalto, J., Pirinen, P., Jylhä, K., 2016. New gridded daily climatology of Finland: Permutation-based uncertainty estimates and temporal trends in climate. J. Geophys. Res. Atmos. 121 (8), 3807–3823. https://doi.org/10.1002/2015JD024651.

Anderson, S.C., Ward, E.J., English, P.A., Barnett, L.A.K., Thorson, J.T., 2022. sdmTMB: An R package for fast, flexible, and user-friendly generalized linear mixed effects models with spatial and spatiotemporal random fields. Ecology. https://doi.org/10.1101/2022.03.24.485545.

Angoh, S.Y.J. (2024). Which environmental factors influence pine marten populations and predation patterns in the boreal forest landscape? [Doctoral thesis, Høgskolen i Innlandet]. In 114. ⟨https://brage.inn.no/inn-xmlui/handle/11250/3132183⟩.

Barros, A.L., Marques, M., Alcobia, S., MacKenzie, D.I., Santos-Reis, M., 2024. Comparing the performance of two camera trap-based methods to survey small mustelids. Basic Appl. Ecol. 75, 18–25. https://doi.org/10.1016/j.baae.2024.01.004.

Bivand, R., Altman, M., Anselin, L., Assunção, R., Bera, A., Berke, O., Blanchet, F.G., Carvalho, M., Christensen, B., Chun, Y., Dormann, C., Dray, S., Dunnington, D., Gómez-Rubio, V., Koley, M., Kossowski, T., Krainski, E., Legendre, P., Lewin-Koh, N., … Yu, D. (2022). R Packages for Analyzing Spatial Data: A Comparative Case Study with Areal Data (Version 1.3-6) [Computer software]. 10.32614/CRAN.package.spdep.

Brainerd, S.M., Rolstad, J., 2002. Habitat selection by Eurasian pine martens Martes martes in managed forests of southern boreal Scandinavia. Wildl. Biol. 8 (4), 289–297. https://doi.org/10.2981/wlb.2002.026.

Cano-Martínez, R., Carricondo-Sanchez, D., Devineau, O., Odden, M., 2021. Small rodent cycles influence interactions among predators in a boreal forest ecosystem. Mammal. Res. 66 (4), 583–593. https://doi.org/10.1007/s13364-021-00590-7.

Crespo-Peremarch, P., Fournier, R.A., Nguyen, V.-T., van Lier, O.R., Ruiz, L.Á., 2020. A comparative assessment of the vertical distribution of forest components using full-waveform airborne, discrete airborne and discrete terrestrial laser scanning data. For. Ecol. Manag. 473, 118268. https://doi.org/10.1016/j.foreco.2020.118268.

Davison, C.W., Assmann, J.J., Normand, S., Rahbek, C., Morueta-Holme, N., 2023. Vegetation structure from LiDAR explains the local richness of birds across Denmark. J. Anim. Ecol. 92 (7), 1332–1344. https://doi.org/10.1111/1365-2656.13945.

Dayal, K.R., Durrieu, S., Alleaume, S., Revers, F., Larmanou, E., Renaud, J.-P., & Bouvier, M. (2020). SCAN ANGLE IMPACT ON LIDAR-DERIVED METRICS USED IN ABA MODELS FOR PREDICTION OF FOREST STAND CHARACTERISTICS: A GRID BASED ANALYSIS. The International Archives of the Photogrammetry, Remote Sensing and Spatial Information Sciences, XLIII-B3-2020, 975–982. XXIV ISPRS Congress, Commission III (Volume XLIII-B3-2020) - 2020 edition. https://doi.org/10.5194/isprs-archives-XLIII-B3-2020-975-2020.

Ecke, F., Löfgren, O., Sörlin, D., 2002. Population dynamics of small mammals in relation to forest age and structural habitat factors in northern Sweden. J. Appl. Ecol. 39 (5), 781–792. https://doi.org/10.1046/j.1365-2664.2002.00759.x.

Finnish Meteorological Institute. (2026). *Seasonal statistics in Finland.* ⟨https://www.ilmatieteenlaitos.fi/vuodenaikojen-tilastot⟩.

Fox, J., Weisberg, S., 2019. An R Companion to Applied Regression, Third edition. Sage, Thousand Oaks CA. https://www.john-fox.ca/Companion/.

Gillies, S. (2018). Rasterio: Geospatial Raster I/O for Python Programmers [Computer software]. ⟨https://github.com/mapbox/rasterio⟩.

Gobakken, T., Næsset, E., 2008. Assessing effects of laser point density, ground sampling intensity, and field sample plot size on biophysical stand properties derived from airborne laser scanner data. Can. J. For. Res. 38 (5), 1095–1109. https://doi.org/10.1139/X07-219.

Hancock, S., Anderson, K., Disney, M., Gaston, K.J., 2017. Measurement of fine-spatial-resolution 3D vegetation structure with airborne waveform lidar: Calibration and validation with voxelised terrestrial lidar. Remote Sens. Environ. 188, 37–50. https://doi.org/10.1016/j.rse.2016.10.041.

Hartig, F., Lohse, L., leite, M. de S., 2022. DHARMa: Residual Diagnostics for Hierarchical (Multi-Level / Mixed) Regression Models (Version 0.4.7) [Computer software]. 10.32614/CRAN.package.DHARMa10.32614/CRAN.package.DHARMa.

Helle, P., Ikonen, K., Kantola, A., 2016. Wildlife monitoring in Finland: Online information for game administration, hunters, and the wider public. Can. J. For. Res. 46 (12), 1491–1496. https://doi.org/10.1139/cjfr-2015-0454.

Herrero, J., Kranz, A., Skumatov, D.V., Abramov, A.V., Maran, T., Monakhov, V.G., 2016. Martes Martes IUCN Red. List Threat. Species 2016, e.T12848A45199169. https://doi.org/10.2305/IUCN.UK.2016-1.RLTS.T12848A45199169.en.

Jordahl, K., Bossche, J.V.D., Fleischmann, M., Wasserman, J., McBride, J., Gerard, J., Tratner, J., Perry, M., Badaracco, A.G., Farmer, C., Hjelle, G.A., Snow, A.D., Cochran, M., Gillies, S., Culbertson, L., Bartos, M., Eubank, N., Maxalbert, Bilogur, A., … Leblanc, F. (2020). *geopandas/geopandas: V0.8.1* (Version v0.8.1) [Computer software]. Zenodo. https://doi.org/10.5281/ZENODO.3946761.

Kane, V.R., McGaughey, R.J., Bakker, J.D., Gersonde, R.F., Lutz, J.A., Franklin, J.F., 2010. Comparisons between field- and LiDAR-based measures of stand structural complexity. Can. J. For. Res. 40 (4), 761–773. https://doi.org/10.1139/X10-024.

Klemola, T., Korpimäki, E., Norrdahl, K., Tanhuanpää, M., Koivula, M., 1999. Mobility and habitat utilization of small mustelids in relation to cyclically fluctuating prey abundances. Ann. Zool. Fenn. 36, 75–82.

Korpela, K., Helle, P., Henttonen, H., Korpimäki, E., Koskela, E., Ovaskainen, O., Pietiäinen, H., Sundell, J., Valkama, J., & Huitu, O. (2014). Predator–vole interactions in northern Europe: The role of small mustelids revised. Proceedings of the Royal Society B: Biological Sciences, 281(1797), 20142119. https://doi.org/10.1098/rspb.2014.2119.

Kotivuori, E., Korhonen, L., Packalen, P., 2016. Nationwide airborne laser scanning based models for volume, biomass and dominant height in Finland. Silva Fenn. 50 (4). ⟨https://www.silvafennica.fi/article/1567⟩.

LAStools. (2025). Efficient LiDAR Processing Software (Versions 17123, academic) [Computer software]. ⟨http://rapidlasso.com/LAStools⟩.

Lindén, A., & Piha, M. (2024). Pienten ja keskikokoisten riistanisäkkäiden kannanmuutokset 1989–2024: Lumijälkilaskentojen tulosraportti (Luonnonvara- ja biotalouden tutkimus 40/2024, p. 20). Luonnonvarakeskus. Helsinki. [In Finnish, with English summary.]. ⟨https://jukuri.luke.fi/handle/11111/9197⟩.

Lindén, H., Helle, E., Helle, P., Wikman, M., 1996. Wildlife triangle scheme in Finland: Methods and aims for monitoring wildlife populations. *Finnish Game.* Research 49, 4–11.

Majasalmi, T., Rautiainen, M., 2020. The impact of tree canopy structure on understory variation in a boreal forest. For. Ecol. Manag. 466, 118100. https://doi.org/10.1016/j.foreco.2020.118100.

LUKE. (2025) The Natural Resources Institute Finland guidelines for field triangle censuses. ⟨https://oma.riistakolmiot.fi/ohje/peltokolmiot⟩.

Martin, R.D., Brabyn, L., Potter, M.A., 2011. Sensitivity of GIS-derived terrain variables at multiple scales for modelling stoat (*Mustela erminea*) activity. Appl. Geogr. 31 (2), 770–779. https://doi.org/10.1016/j.apgeog.2010.08.005.

McDonald, R.A., Abramov, A.V., Stubbe, M., Herrero, J., Maran, T., Tikhonov, A., Cavallini, P., Kranz, A., Giannatos, G., Kryštufek, B., Reid, F., 2019. Mustela nivalis (amended version of 2016 assessment). IUCN Red. List Threat. Species 2019, e.T70207409A147993366. https://doi.org/10.2305/IUCN.UK.2016-1.RLTS.T70207409A147993366.en.

McElhinny, C., Gibbons, P., Brack, C., Bauhus, J., 2005. Forest and woodland stand structural complexity: Its definition and measurement. For. Ecol. Manag. 218 (1), 1–24. https://doi.org/10.1016/j.foreco.2005.08.034.

Mergey, M., Helder, R., Roeder, J.-J., 2011. Effect of forest fragmentation on space-use patterns in the European pine marten (Martes martes. J. Mammal. 92 (2), 328–335. https://doi.org/10.1644/09-MAMM-A-366.1.

Mergey, M., Kaerle, C., Helder, R., 2023. Variations in density of pine marten Martes martes populations according to forest fragmentation. Mammal. Res. 68 (4), 507–519. https://doi.org/10.1007/s13364-023-00704-3.

National Land Survey of Finland. (2025a). Laser scanning data 0,5 p. ⟨https://www.maanmittauslaitos.fi/en/maps-and-spatial-data/datasets-and-interfaces/product-descriptions/laser-scanning-data-05-p⟩.

National Land Survey of Finland. (2025b). Laser scanning data 0,5 p (2008-2019). ⟨https://www.maanmittauslaitos.fi/en/maps-and-spatial-data/datasets-and-interfaces/product-descriptions/laser-scanning-data⟩.

Nilsson, M.-C., Wardle, D.A., 2005. Understory vegetation as a forest ecosystem driver: Evidence from the northern Swedish boreal forest. Front. Ecol. Environ. 3 (8), 421–428. https://doi.org/10.1890/1540-9295(2005)003%255B0421:UVAAFE%255D2.0.CO;2.

Paton, R.S., Matthiopoulos, J., 2016. Defining the scale of habitat availability for models of habitat selection. Ecology 97 (5), 1113–1122. https://doi.org/10.1890/14-2241.1.

Perry, M.T. (2017). Rasterstats [Computer software]. ⟨https://github.com/perrygeo/python-rasterstats⟩.

Reid, F., Helgen, K., Kranz, A., 2015. Mustela erminea: The IUCN Red List of Threatened Species. 2016(e.T29674A45203335). https://doi.org/10.2305/IUCN.UK.2016-1.RLTS.T29674A45203335.en.

Rouault, E., Warmerdam, F., Schwehr, K., Kiselev, A., Butler, H., Łoskot, M., Szekeres, T., Tourigny, E., Landa, M., Miara, I., Elliston, B., Chaitanya, K., Plesea, L., Morissette, D., Jolma, A., Dawson, N., Baston, D., de Stigter, C., & Miura, H. (2025). GDAL (Version v3.12.0beta1) [Computer software]. Zenodo. https://doi.org/10.5281/ZENODO.17400423.

R Core Team, 2024. R: A Language and Environment for Statistical Computing. R Foundation for Statistical Computing, Vienna, Austria. https://www.R-project.org/.

Savola, S., Henttonen, H., Lindén, H., 2013. Vole Population Dynamics During the Succession of a Commercial Forest in Northern Finland. Ann. Zool. Fenn. 50 (1–2), 79–88. https://doi.org/10.5735/086.050.0107.

Sidorovich, V.E., Polozov, A.G., Solovej, I.A., 2008. Niche separation between the weasel Mustela nivalis and the stoat M. erminea in Belarus. Wildl. Biol. 14 (2), 199–210. https://doi.org/10.2981/0909-6396(2008)14%255B199:NSBTWM%255D2.0.CO;2.

Toivonen, J., Kangas, A., Maltamo, M., Kukkonen, M., Packalen, P., 2023. Assessing biodiversity using forest structure indicators based on airborne laser scanning data. For. Ecol. Manag. 546, 121376. https://doi.org/10.1016/j.foreco.2023.121376.

Tweedy, P.J., Moriarty, K.M., Bailey, J.D., Epps, C.W., 2019. Using fine scale resolution vegetation data from LiDAR and ground-based sampling to predict Pacific marten resting habitat at multiple spatial scales. For. Ecol. Manag. 452, 117556. https://doi.org/10.1016/j.foreco.2019.117556.

Twining, J.P., Montgomery, I., Fitzpatrick, V., Marks, N., Scantlebury, D.M., Tosh, D.G., 2019. Seasonal, geographical, and habitat effects on the diet of a recovering predator population: The European pine marten (Martes martes) in Ireland. Eur. J. Wildl. Res. 65 (3), 51. https://doi.org/10.1007/s10344-019-1289-z.

Twining, J.P., Montgomery, W.I., Reid, N., Marks, N., Tosh, D.G., Scantlebury, D.M., 2020. All forests are not equal: Population demographics and denning behaviour of a recovering small carnivore in human modified landscapes. Wildl. Biol. 2020(4) wlb 00760. https://doi.org/10.2981/wlb.00760.

Wegge, P., Rolstad, J., 2018. Cyclic small rodents in boreal forests and the effects of even-aged forest management: Patterns and predictions from a long-term study in southeastern Norway. For. Ecol. Manag. 422, 79–86. https://doi.org/10.1016/j.foreco.2018.04.011.

Wheelhouse, L., Bryan, H., Crowley, S., Johnson, C., Hodder, D., 2025. Riparian Areas and Fine-Scale Forest Cover and Structure Drive Occupancy Patterns of Sympatric Mustelids. Ecol. Evol. 15 (5), e71370. https://doi.org/10.1002/ece3.71370.

White, J.C., Coops, N.C., Wulder, M.A., Vastaranta, M., Hilker, T., Tompalski, P., 2016. Remote Sensing Technologies for Enhancing Forest Inventories: A Review. Can. J. Remote Sens. 42 (5), 619–641. https://doi.org/10.1080/07038992.2016.1207484.

Willebrand, T., Willebrand, S., Jahren, T., Marcström, V., 2017. Snow tracking reveals different foraging patterns of red foxes and pine martens. Mammal. Res. 62 (4), 331–340. https://doi.org/10.1007/s13364-017-0332-2.

Wright, P.G.R., Croose, E., Macpherson, J.L., 2022. A global review of the conservation threats and status of mustelids. Mammal. Rev. 52 (3), 410–424. https://doi.org/10.1111/mam.12288.

Ylönen, H., Haapakoski, M., Sievert, T., Sundell, J., 2019. Voles and weasels in the boreal Fennoscandian small mammal community: What happens if the least weasel disappears due to climate change. Integr. Zool. 14 (4), 327–340. https://doi.org/10.1111/1749-4877.12388.

Zhou, Y.-B., Newman, C., Xu, W.-T., Buesching, C.D., Zalewski, A., Kaneko, Y., Macdonald, D.W., Xie, Z.-Q., 2011. Biogeographical variation in the diet of Holarctic martens (genus Martes, Mammalia: Carnivora: Mustelidae): adaptive foraging in generalists. J. Biogeogr. 38 (1), 137–147. https://doi.org/10.1111/j.1365-2699.2010.02396.x.

Zub, K., Sönnichsen, L., Szafrańska, P.A., 2008. Habitat requirements of weasels Mustela nivalis constrain their impact on prey populations in complex ecosystems of the temperate zone. Oecologia 157 (4), 571–582. https://doi.org/10.1007/s00442-008-1109-8.

Zuur, A.F., Ieno, E.N., Elphick, C.S., 2010. A protocol for data exploration to avoid common statistical problems. Methods Ecol. Evol. 1 (1), 3–14. https://doi.org/10.1111/j.2041-210X.2009.00001.x.